

A Comparative Quantitative Proteomic Study Identifies New Proteins Relevant for Sulfur Oxidation in the Purple Sulfur Bacterium *Allochromatium vinosum*

Thomas Weissgerber,^a Marc Sylvester,^b Lena Kröninger,^a Christiane Dahl^a

Institut für Mikrobiologie & Biotechnologie, Rheinische Friedrich-Wilhelms-Universität Bonn, Bonn, Germany^a; Institut für Biochemie und Molekularbiologie, Rheinische Friedrich-Wilhelms-Universität Bonn, Bonn, Germany^b

In the present study, we compared the proteome response of *Allochromatium vinosum* when growing photoautotrophically in the presence of sulfide, thiosulfate, and elemental sulfur with the proteome response when the organism was growing photoheterotrophically on malate. Applying tandem mass tag analysis as well as two-dimensional (2D) PAGE, we detected 1,955 of the 3,302 predicted proteins by identification of at least two peptides (59.2%) and quantified 1,848 of the identified proteins. Altered relative protein amounts (≥ 1.5 -fold) were observed for 385 proteins, corresponding to 20.8% of the quantified *A. vinosum* proteome. A significant number of the proteins exhibiting strongly enhanced relative protein levels in the presence of reduced sulfur compounds are well documented essential players during oxidative sulfur metabolism, e.g., the dissimilatory sulfite reductase DsrAB. Changes in protein levels generally matched those observed for the respective relative mRNA levels in a previous study and allowed identification of new genes/proteins participating in oxidative sulfur metabolism. One gene cluster (*hyd*; Alvin_2036-Alvin_2040) and one hypothetical protein (Alvin_2107) exhibiting strong responses on both the transcriptome and proteome levels were chosen for gene inactivation and phenotypic analyses of the respective mutant strains, which verified the importance of the so-called Isp hydrogenase supercomplex for efficient oxidation of sulfide and a crucial role of Alvin_2107 for the oxidation of sulfur stored in sulfur globules to sulfite. In addition, we analyzed the sulfur globule proteome and identified a new sulfur globule protein (SgpD; Alvin_2515).

Sulfur-oxidizing bacteria and archaea are metabolically and phylogenetically very diverse and occur in a wide range of habitats (1). Aerobic and facultatively anaerobic chemotrophic sulfur oxidizers typically inhabit ecosystems that feature opposing gradients of their sulfur substrates and oxygen or nitrate. These gradients are often very steep. In addition, if light is available, phototrophic sulfur bacteria catalyze anaerobic oxidation of reduced sulfur compounds. Sulfur oxidizers play a crucial ecological role in the global sulfur cycle by reoxidizing sulfide released by sulfate-reducing bacteria in deeper anoxic layers or arising from geothermal activity. The great diversity of sulfur-oxidizing prokaryotes is reflected by the fact that a universal mechanism for the oxidation of sulfur compounds does not exist. However, a significant number of environmentally very important organisms pursue the Dsr pathway of sulfur oxidation (1, 2). These include not only the anoxygenic phototrophic purple and green sulfur bacteria but also many chemolithotrophic sulfur oxidizers, such as the giant bacteria *Beggiatoa*, *Thioploca*, and *Thiomargarita* or the endosymbionts of marine invertebrates. This pathway includes the formation of zero-valent sulfur as a characteristic intermediate. The sulfur is deposited either extracellularly or within the confines of the bacterial cells, depending on the group to which the organisms belong.

Purple sulfur bacteria are comparatively well-studied examples employing the rather complex oxidative Dsr pathway. Most insights about this pathway were obtained from enzyme assays and sequence analysis of specific gene clusters in *Allochromatium vinosum* DSM 180^T, a gammaproteobacterium of the family *Chromatiaceae*. The organism is metabolically versatile. Phototrophic growth using sunlight as the energy source and reduced sulfur compounds (e.g., sulfide, polysulfides, thiosulfate, and elemental

sulfur) as the electron donors for carbon dioxide fixation via the Calvin cycle is its primary and most characteristic metabolic trait. However, organoheterotrophic growth of this organism on organic acids like malate or pyruvate is also possible (3). *A. vinosum* has been adopted as a model organism for laboratory-based studies of oxidative sulfur metabolism. Cultivation is comparatively easy, the organism is genetically accessible (4, 5), the complete genomic sequence is available (6), and a system for complementation of mutations exists (7–9).

In *A. vinosum*, the oxidation of sulfide is catalyzed in the periplasm by flavocytochrome *c* (FccAB) and two different sulfide:quinone oxidoreductases (SqrD and SqrF) (10, 11). Thiosulfate is fed into the Dsr pathway by the periplasmic Sox proteins (SoxXAK, SoxYZ, SoxB, and SoxL) (2, 6, 9, 12, 13). The periplasmic sulfur globules that are formed as the products of these oxidative processes are enclosed by a monolayered hydrophobic protein envelope. So far, three different hydrophobic structural proteins, namely, SgpA, SgpB, and SgpC, are known to constitute this envelope (14, 15). SgpA and SgpB are very similar in amino acid sequence and can functionally replace each other. SgpC par-

Received 19 December 2013 Accepted 25 January 2014

Published ahead of print 31 January 2014

Editor: G. Voordouw

Address correspondence to Christiane Dahl, chdahl@uni-bonn.de.

Supplemental material for this article may be found at <http://dx.doi.org/10.1128/AEM.04182-13>.

Copyright © 2014, American Society for Microbiology. All Rights Reserved.

doi:10.1128/AEM.04182-13

ticipates in sulfur globule expansion (16). A complicated mechanism that requires the presence of many different enzymes encoded in the *dsr* gene cluster is necessary for oxidation of stored sulfur (17, 18). Low-molecular-weight organic persulfides, possibly glutathione or glutathione amide persulfide, have been proposed to be carrier molecules transferring sulfur from the periplasmic sulfur globules into the cytoplasm. Here, a sulfur relay system sets in that starts with the sulfur-mobilizing rhodanese-like protein Rhd_2599 (Alvin_2599). This enzyme then transfers the sulfur from the low-molecular-weight thiol to the TusA protein (Alvin_2600). TusA serves as a sulfur donor for DsrEFH, which persulfurates DsrC. The latter very probably serves as a direct substrate for reverse-acting sulfite reductase, DsrAB (19–21; Y. Stockdreher, M. Sturm, M. Josten, H. G. Sahl, N. Dobler, R. Zigann, and C. Dahl, submitted for publication). The product of the oxidative step catalyzed by DsrAB is sulfite, which is oxidized to the final product, sulfate, either directly via the membrane-bound iron-sulfur molybdoprotein SoeABC or by an indirect pathway involving formation of adenosine-5-phosphosulfate (APS) catalyzed by APS reductase and ATP sulfurylase (5, 22, 23).

Although the model describing the major steps of sulfur oxidation in *A. vinosum* was significantly refined recently (2, 13, 19), many questions are still open. These include questions of how sulfur gets in and out of the sulfur globules, how sulfur is transported into the cytoplasm, and how elemental sulfur, when present as an extracellular, virtually water-insoluble substrate, is attacked enzymatically for oxidation. To answer these questions, we are presently seeking to develop a more comprehensive and coherent picture of sulfur oxidation and bioenergetic processes in *A. vinosum*. We started with whole-genome transcriptional profiling of the responses of *A. vinosum* to the presence of four different reduced sulfur compounds. This approach has already allowed the identification of new genes that encode proteins with appropriate subcellular localization and properties for participating in oxidative dissimilatory sulfur metabolism (13). In the present study, we expanded our global investigations to the level of the proteome and performed whole-proteome profiling of the photoautotrophic response of *A. vinosum* to the presence of sulfide, thiosulfate, or elemental sulfur and compared its photoheterotrophic response to malate. Furthermore, we enriched and analyzed the sulfur globule proteome in order to elucidate the possibility that enzymes taking part in sulfur globule formation and/or oxidation are bound to or interact with the envelope proteins, similar to the situation found for polyhydroxyalkanoate (PHA) granules (24). In addition, we chose one single gene and one gene cluster exhibiting a conspicuous behavior in both the transcriptomic and proteomic profiling approaches for inactivation and phenotypic analyses of the respective mutant strains. This strategy indeed confirmed the importance of the encoded proteins for formation/degradation of sulfur globules and thereby also documented the suitability of comparative proteomics for the identification of further new sulfur-related genes in anaerobic phototrophic sulfur bacteria.

MATERIALS AND METHODS

Bacterial strains, plasmids, growth conditions, and recombinant DNA techniques. Bacterial strains and plasmids used in this study are listed in Table S1 in the supplemental material. *Allochrochromatium vinosum* DSM 180^T wild-type and mutant cells were cultivated photolithoautotrophically in batch culture at 30°C under anaerobic conditions and continuous

illumination in completely filled screw-cap culture bottles containing modified Pfenning's medium ("0" medium without sulfide) (9). All media contained 1 g liter⁻¹ ammonium chloride. Sulfide (4 mM or 8 mM), thiosulfate (4 mM or 10 mM), sulfite (5 mM), or sulfur (50 mM) was added to the cultures as a sulfur source. For photoorganoheterotrophic growth on malate (22 mM) with sulfate as the only sulfur source, MgCl₂ was replaced by MgSO₄. Cells of *A. vinosum*, grown photoorganoheterotrophically on malate (RCV medium [25]) for 3 days, were used as an inoculum for growth experiments. The volume of the cultures grown for inoculum preparation was 250 or 500 ml. Inoculum cells were harvested by centrifugation (10 min, 2,680 × g) and washed once in "0" medium. For two-dimensional (2D) PAGE experiments, cells were cultivated in a volume of 250 ml RCV or "0" medium supplemented with the respective sulfur source. These cultures were inoculated with stationary-phase cells taken from 125 ml of inoculum-preparation cultures. Cells were harvested 8 h after inoculation when malate, sulfide (4 mM), or thiosulfate (10 mM) was the substrate. In contrast to the oxidation of sulfide and thiosulfate, where sulfur globules appear inside the cells minutes after inoculation, oxidation of elemental sulfur first requires uptake of this virtually water-insoluble substrate. Sulfur globules start to appear about 3 h after inoculation of a culture with elemental sulfur (26). Hence, the incubation period was prolonged accordingly, and cells were harvested after 24 h when elemental sulfur (50 mM) was the electron donor. In a second run, incubation on reduced sulfur compounds was extended. After 24 h, cells grown on the different sulfur sources were harvested and transferred into fresh medium containing the respective sulfur compound, and incubation was continued for an additional 8 h on sulfide or thiosulfate or for 24 h on elemental sulfur. For tandem mass tag experiments, two independent culture replicates were run for each condition in 250 ml of "0" medium supplemented with malate or a particular reduced sulfur compound and harvested 8 h after inoculation into sulfide or thiosulfate medium and 24 h after inoculation into elemental sulfur medium. These cultures were inoculated with stationary-phase cells taken from 125-ml precultures. The culture volume for phenotypic analyses of wild-type and mutant strains was 250 ml. In these experiments, the starting optical density at 690 nm (OD₆₉₀) was set to 0.8 to 0.9. *Escherichia coli* strains were cultured in LB medium (27). Antibiotics were used in the following concentrations (in μg ml⁻¹): for *E. coli*, ampicillin, 100; kanamycin, 50; for *A. vinosum*, ampicillin, 20; kanamycin, 10; rifampin, 50. Recombinant DNA techniques were performed as described earlier (13).

Construction and analysis of *A. vinosum* ΔAlvin_2036-2040::ΩKm and ΔAlvin_2107::ΩKm strains. For the replacement of gene cluster Alvin_2036-Alvin_2040 and gene Alvin_2107, respectively, in the genome of *A. vinosum* by an Ω kanamycin cassette, splicing by overlap extension (SOE) PCR fragments were constructed using primers MBH-KO-P1 to MBH-KO-P4 and Del-Alvin2107_1 to Del-Alvin2107_4, respectively (see Table S1 in the supplemental material) (28). The fragments were inserted into the mobilizable plasmid pSUP301 (29) and into pASK-IBA5plus by HindIII restriction sites, resulting in plasmids pSUP301-Del2036-2040 and pASK-IBA5plus-Del2107. The kanamycin cassette of plasmid pHP45ΩKm was integrated into these plasmids via EcoRI restriction sites in the case of pSUP301-Del2036-2040 and via BamHI restriction sites in the case of pASK-IBA5plus-Del2107. The Del2107Km fragment of pASK-IBA5plus-Del2107 was amplified using primers IBA-2107+ KanFor and -Rev and inserted into plasmid pSUP301 by ClaI restriction sites. The final mobilizable constructs pSUP301-Del2036-2040Km and pSUP301-Del2107Km were transferred from *E. coli* S17.1 to *A. vinosum* Rif50 by conjugation (4). Transconjugants were selected on RCV plates containing the appropriate antibiotics under anoxic conditions in the light. Double crossover recombinants lost the vector-encoded ampicillin resistance. The genotype of double crossover recombinants was finally verified by Southern hybridization experiments. Sulfur compounds were analyzed as described earlier (13). For quantification of sulfur compounds, a volume up to 2 ml was taken from the culture bottles and immediately replaced by fresh medium to maintain anaerobiosis.

Two-dimensional polyacrylamide gel electrophoresis. Cells from 125-ml cultures were harvested ($12,800 \times g$, 10 min, 4°C), washed twice in PBS buffer (140 mM NaCl, 10 mM $\text{Na}_2\text{HPO}_4 \cdot 2\text{H}_2\text{O}$, 2.7 mM KCl, and 1.8 mM KH_2PO_4) and once in Tris-buffered sucrose washing solution (10 mM Tris-HCl [pH 7.0] and 250 mM sucrose) ($12,800 \times g$, 10 min, 4°C). Cell pellets were stored at -80°C . The pellets were resuspended in lysis buffer (40 μl 50-fold-concentrated cOmplete protease inhibitor [Roche, Mannheim, Germany], 60 μl 150 mM phenylmethylsulfonyl fluoride [PMSF] in isopropanol, and 20 μl 1 M Tris-HCl [pH 8.0], brought up to 1,800 μl with double-distilled water [ddH_2O]). A volume of 600 μl of the resuspended cells was transferred to 1.5-ml reaction tubes filled with 250-ng zirconium glass beads (diameter, 0.1 mm) for cell lysis (15 s, Ivoclar Vivadent Silamat S6; Ivoclar Vivadent AG, Schaan, Lichtenstein). Cell debris and glass beads were removed by centrifugation ($16,200 \times g$, 5 min, 4°C). For DNA and RNA digestion, 200 μl RNase/DNase solution (0.25 mg ml^{-1} RNase [90 U mg^{-1}] and 1 mg ml^{-1} DNase I [400 U mg^{-1}] in 50 mM MgCl_2) was added to the lysate and incubated at 4°C for 1 h. Remaining cells, cell debris, and glass beads were removed by a further centrifugation step ($16,200 \times g$, 20 min, 4°C). For the preparation of the “soluble” protein fraction, extracts were subjected to ultracentrifugation ($145,000 \times g$, 3 h, 4°C) in urea-thiourea buffer (8 M urea, 2 M thiourea, 2% [wt/vol] 3-[(3-cholamidopropyl)dimethylammonio]-1-propanesulfonate [CHAPS], 1% [wt/vol] dithiothreitol [DTT], 0.2% ampholytes, 4.5 mM PMSF, and 1 \times cOmplete protease inhibitor [Roche, Mannheim, Germany]). The solubilized proteins of the supernatant were precipitated by chloroform-methanol precipitation. The pellets were dried with nitrogen and resolubilized in rehydration buffer (8 M urea, 2 M thiourea, 1% [wt/vol] CHAPS, 0.3% [wt/vol] DTT, 10% [vol/vol] glycerol, and 0.5% ampholytes). Insoluble components were removed by centrifugation ($16,200 \times g$, 20 min, 16°C), and the protein solution was stored at -20°C . The protein concentration was determined using the Roti-Nanoquant assay (Roth, Karlsruhe, Germany). A 1- μl sample was added to 19 μl rehydration buffer and mixed with 1 ml Nanoquant working solution. After 5 min of incubation at room temperature (RT), absorption was measured against a reagent blank at 595 nm. The measurement was calibrated with bovine serum albumin in rehydration buffer. A mixture of 300 μl rehydration buffer containing 300 μg protein and 1.5 μl IPG buffer (GE Healthcare, Munich, Germany) (pH 4 to 7) was centrifuged and transferred onto the focusing tray of the Protean IEF cell (Bio-Rad, Munich, Germany) for active rehydration of the ReadyStrip immobilized pH gradient (IPG) strips (pH 4 to 7) (Bio-Rad, Munich, Germany). Samples were covered with silicon oil to avoid dehydration. Active rehydration was performed at 50 V for 16 h at 20°C , followed by separation in the first dimension via isoelectric focusing at 20°C (200 V rapid for 2 h, 500 V rapid for 2 h, 1,000 V linear for 10 min, 1,000 V for 1.5 h, 10,000 V linear for 40 min, 10,000 V for 7 h, and 1,000 V rapid for 24 h). Focused IPG strips were equilibrated in equilibration solution (6 M urea, 30% [vol/vol] glycerol, 50 mM Tris-HCl [pH 8.8], 2% [wt/vol] SDS, and 0.01% [wt/vol] bromophenol blue) supplemented with 1% (wt/vol) DTT for 20 min in a first step and supplemented with 5% (wt/vol) iodoacetamide (IAA) for 20 min in a second step. After equilibration, separation in the second dimension was carried out using 15% SDS-polyacrylamide gels in a Protean II XL cell (Bio-Rad, Munich, Germany). IPG strips were fixed onto the SDS gels with 0.7% (wt/vol) agarose (NEEO ultra-quality; Roth, Karlsruhe, Germany) dissolved in running buffer (30). During the first 2 h, proteins were separated at a maximum of 0.2 W at 5 mA, and then power was increased to a maximum of 15 W at 40 mA. The gels were stained in Coomassie solution [0.1% (wt/vol) Coomassie brilliant blue G-250, 1.3 M $(\text{NH}_4)_2\text{SO}_4$, 0.5% (vol/vol) acetic acid, and 34% (vol/vol) methanol] and destained in water supplemented with 2% (vol/vol) acetic acid. SDS-PAGE was carried out in duplicate for the protein samples generated from photoorganoheterotrophically grown cells and in triplicate for the protein samples generated from photolithoautotrophically grown *A. vinosum* cells. The gels were scanned using the Molecular Imager FX instrument (Bio-Rad, Munich, Germany), and the protein spots were analyzed using the software program PDQuest (Bio-

Rad, Munich, Germany). Background subtraction, normalization (total density in gel image), and statistical analysis (Student's *t* test) were automatically carried out by the software program.

Quantification via tandem mass tags. For peptide preparation, cells from 250-ml cultures were harvested ($12,800 \times g$, 10 min, 4°C) and washed once in Tris-EDTA (TE) buffer (10 mM Tris [pH 8.0] and 10 mM EDTA). Washed cells were resuspended in 5 ml TE buffer and disrupted by sonication (Cell Disruptor B15; Branson) for 1.5 min ml^{-1} at 4°C . Cell debris was removed by centrifugation ($16,200 \times g$, 20 min, 4°C). The supernatant (crude extract) was subjected to ultracentrifugation ($145,000 \times g$, 3 h, 4°C). The supernatant after centrifugation contained the soluble protein fraction. Each pellet containing the membrane protein fraction was resuspended in 5 ml TE buffer containing 2% (wt/vol) SDS. For more effective solubilization of the membrane proteins, the solution was stirred for 30 min at room temperature. Both the soluble protein fraction and the solubilized membrane fraction were subjected to in-solution-preparation of peptides on centrifugal filter units modified as described elsewhere (31–34). In brief, solutions containing 100 μg protein were reduced with 20 mM DTT at 55°C for 20 min and loaded onto centrifugal filter units with a 10-kDa-cutoff modified polyethersulfone (PES) membrane (Pall Filtersystems, Crailsheim, Germany). The buffer was exchanged by centrifugation and addition of 20 mM triethylammonium bicarbonate (TEAB)–0.5% sodium deoxycholate (SDC). Alkylation of thiol groups was done with 40 mM IAA for 20 min at room temperature in the dark. After another buffer exchange, 1 μg trypsin was added to 20 mM TEAB–0.5% SDC in a total volume of 50 μl . Digestion proceeded overnight at 37°C . Peptides were collected, and SDC was precipitated with trifluoroacetic acid (TFA) (0.5%, final). The remaining SDC was removed by phase transfer with an equal volume of ethyl acetate. Peptides were vacuum concentrated and labeled with amine-reactive, 6-plex tandem mass tag reagents (Thermo Fisher Scientific, Bonn, Germany) according to the manufacturer's instructions. The labeling reaction was quenched by addition of 5% hydroxylamine. Labeled peptides were pooled and desalted on Oasis HLB cartridges (Waters GmbH, Eschborn, Germany). Eluates containing 70% acetonitrile and 0.1% formic acid (FA) were dried and fractionated to 24 fractions by isoelectric point with an Offgel fractionator (Agilent Technologies, Waldbronn, Germany). Peptide fractions were dried and stored at -20°C .

For LC-MS measurements, peptides were dissolved in 8 μl 0.1% FA (solvent A). A 1.6- μl volume was injected onto a C_{18} trap column (20-mm length, 100- μm inner diameter, ReproSil-Pur 120 C18-AQ, 5 μm ; Dr. Maisch GmbH, Ammerbuch-Entringen, Germany) made in-house. Bound peptides were eluted onto a C_{18} analytical column (200-mm length, 75- μm inner diameter, ReproSil-Pur 120 C18-AQ, 1.9 μm). Peptides were separated during a linear gradient from 3% to 55% solvent B (80% acetonitrile and 0.1% formic acid) within 80 min at 350 nl/min. The nano-HPLC instrument was coupled online to an LTQ Orbitrap Velos mass spectrometer (Thermo Fisher Scientific, Bremen, Germany). Peptide ions between 380 and 1,850 m/z were scanned in the Orbitrap detector with a resolution of 30,000 (maximum fill time, 400 ms; automatic gain control [AGC] target, 10^6). The 12 most intense precursor ions (threshold intensity, 5,000) were subjected to collision-induced dissociation (at a setting of 34% normalized energy), and fragments were analyzed in the linear ion trap. The same 12 precursors were then isolated and fragmented by higher collision dissociation (HCD) (normalized energy, 42%) and analyzed in the Orbitrap detector ($R = 7,500$). Fragmented peptide ions were excluded from repeat analysis for 15 s.

Raw data processing and analysis of database searches were performed using the Proteome Discoverer 1.4.0.288 software program (Thermo Fisher Scientific). Peptide identification was done with an in-house Mascot server, version 2.4 (Matrix Science Ltd., London, United Kingdom). MS2 data were searched against ALLVD sequences from NCBIInr (release 2012_07). Precursor ion m/z tolerance was 12 ppm, and fragment ion tolerance was 0.5 Da (collision-induced dissociation [CID]) and 20 millimass units (mmu) (HCD), respectively. Fragment ion data were searched

using b and y ions. Additionally, a ions were included for HCD spectra. Tryptic peptides with up to one missed cleavage were searched. Carbamidomethylation of cysteines and tandem mass tag (TMT) modification of lysines and peptide N termini were set as static modifications. Oxidation was allowed as a dynamic modification of methionine. Mascot results were assigned posterior error probabilities (PEP) by the percolator algorithm (Kall et al., 2008), version 1.17, as implemented in the software program Proteome Discoverer. Spectra with identifications below 1% PEP were sent to a second round of database search with semitryptic enzyme specificity (one missed cleavage allowed). Dynamic modifications were carbamidomethylation (cysteine), oxidation (methionine) and pyroglutamate (glutamate, glutamine), along with TMT as a modification group. Proteins were included if at least two peptides were identified with a PEP of <1%. Quantification was performed with Proteome Discoverer software using HCD spectra only. Compression of quantification ratios due to cofragmented peptides was reduced by excluding peptides with >30% foreign peptides in the isolation window. Peptide ratios were normalized by the median ratio for each channel. Only unique peptides were included in protein quantification. Furthermore, *P* values were calculated by a two-tailed, two-sample Student *t* test assuming unequal variances (Excel; Microsoft Office), comparing the relative protein levels of a protein in the replicates to the relative protein levels of all proteins in the replicates and conditions. In order to gain information about the relative abundance of each protein in the cell, we formed the ratio between the number of peptide spectrum matches and the number of amino acids of the respective protein. We thus avoided overestimation of large proteins and underestimation of small proteins.

Enrichment of the sulfur globule proteome. For enrichment of the sulfur globule proteome, cells of *A. vinosum* wild type and *A. vinosum* Δ *dsrJ* were cultivated in a volume of 1 liter “0” medium supplemented with sulfide (6 mM). The Δ *dsrJ* strain was especially well suited for this purpose because it accumulates massive amounts of sulfur globules due to its complete inability to form sulfite from stored sulfur (35). Preparation of the sulfur globules and separation of the proteins associated with them in one dimension via SDS-PAGE were performed as described by Brune (14). Proteins were in-gel digested with trypsin, followed by mass spectrometric analysis. Those proteins that gave rise to at least seven-times-higher total numbers of relative peptide spectrum matches in the sulfur globule proteome than in the proteome of sulfide-grown cells were considered enriched.

Tryptic in-gel digestion of proteins prior to mass spectrometric analysis. Tryptic digestion of proteins in PAGE bands obtained from 1- and 2-dimensional PAGE was performed as previously described (36, 37). Briefly, lanes of one-dimensional SDS-PAGE gels were cut into 10 to 15 slices with 2- to 3-mm heights. The slices were transferred into 0.5-ml reaction tubes and cut into 1-mm² pieces with a pipette tip. Gel pieces were washed once in 100 μ l 50% (vol/vol) acetonitrile (ACN) (shaking for 1 min at RT), followed by shrinking of the gel in 100 μ l 100% ACN (shaking for 5 min, RT). ACN was removed, and the remaining moisture was evaporated by incubation at 60°C for 10 min. For reduction and alkylation of thiol groups, gel pieces were swelled in 50 μ l DTT (10 mM in 0.1 M NH₄HCO₃) for 30 min at 55°C, followed by removal of the solution and addition of 50 μ l IAA (55 mM in 0.1 M NH₄HCO₃) and a further incubation step for 30 min at RT in the dark. IAA solution was removed, and gel pieces were washed in 100 μ l 50% ACN (shaking for 5 min, RT) and shrunk completely in 100 μ l 100% ACN (shaking for 5 min, RT). ACN was removed, and gel pieces were dried completely using a SpeedVac instrument. For tryptic in-gel digestion, 20 μ l trypsin solution (16.7 ng/ μ l T6567, proteomics grade [Sigma-Aldrich, Munich, Germany], in 50 mM NH₄HCO₃-9% ACN) and 50 μ l 50 mM NH₄CO₃ were added and incubated overnight at 37°C. Supernatant was transferred into a new tube, vacuum dried, and stored at -20°C until analysis via mass spectrometry. 2D gel spots were treated the same way.

RESULTS AND DISCUSSION

Two-dimensional gel electrophoresis. Transcription profiles obtained previously for *A. vinosum* provided global insights into changes in relative mRNA levels triggered by reduced sulfur compounds. Important roles of established pathways were confirmed, and new sulfur-metabolism related genes were identified (13). However, changes in gene expression at the RNA level may be only transient and do not always lead to changes in protein composition. We therefore first surveyed differences between the protein array of *A. vinosum* cells grown photoorganoheterotrophically on malate and that of *A. vinosum* cells grown photolithoautotrophically on reduced sulfur compounds (4 mM sulfide or 10 mM thio-sulfate for 8 h or 50 mM elemental sulfur for 24 h) at exactly the same light intensity by a classical two-dimensional gel electrophoresis approach using 15% SDS-PAGE gels in the second dimension to guarantee optimum separation of low-molecular-weight proteins. The chosen incubation periods correspond to those at which *A. vinosum* had already oxidized a major portion of the supplied sulfur source and revealed constant sulfate production rates (see Fig. S1 in the supplemental material). It should be pointed out that samples for quantification of sulfur compounds and samples harvested for proteomic analyses were not taken from the same culture bottles. However, these cultures were incubated in parallel under the same conditions. As can be inferred from the very small error bars calculated for the experiments shown in Fig. S1, there was hardly any variation between parallel cultures. We can therefore confidently state that the cells subjected to proteomic analyses were in the same stage of metabolism/growth as those in the cultures shown in Fig. S1. We detected more than 600 individual protein spots originating from proteins with isoelectric points between pH 4 and 7 (Fig. 1) and identified 138 of these by mass spectrometry of tryptic peptides (see Fig. S2). The general protein composition of *A. vinosum* cells did not change dramatically upon the switch from malate to a reduced sulfur compound and carbon dioxide. In Fig. 1, gels for malate- and sulfide-grown cells are shown as examples. The most prominent spots appeared to be the same under all growth conditions. In actively growing cells, ribosomal proteins and ancillary components are usually highly abundant (38, 39). Accordingly, one of the most prominent spots we identified originated from elongation factor EF-TU (Alvin_2365). Not surprisingly, high-potential iron-sulfur protein (HiPIP), the primary electron donor to the photosynthetic reaction center in *A. vinosum* (40), also formed a noticeable spot as did malic enzyme (Alvin_3051), which feeds malate into central carbon metabolism in *A. vinosum* via the formation of pyruvate (41). Several proteins with established functions in oxidative sulfur metabolism or subunits thereof were also readily detected. These included FccB, the FAD binding subunit of flavocytochrome *c* sulfide dehydrogenase (10), SoxL (12), DsrC, and also TusA. Only very recently, we identified the latter as an important part of a relay system delivering sulfur to DsrC (Stockdreher et al., submitted), which finally presents it as a substrate for oxidation by the reverse-acting dissimilatory sulfite reductase DsrAB (19, 20, 42). Comparison of the 2D gels showed that changes in relative mRNA levels (13) are at least in part mirrored at the protein level in the purple sulfur bacterium. Both subunits of the major RuBisCO species (RbcA and RbcB) in *A. vinosum* increased significantly in amount upon autotrophic growth. The same was true for the DsrA subunit of sulfite reductase, while the

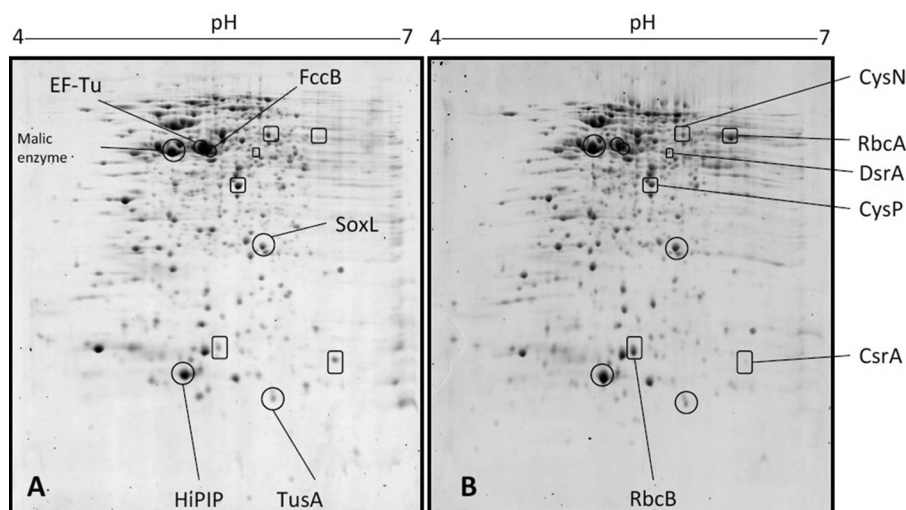


FIG 1 2D display of soluble proteins of *Allochrochromatium vinosum* cells grown on 22 mM malate (A) or 4 mM sulfide (B). Highly abundant proteins (circles) and proteins exhibiting especially conspicuous changes in spot intensities (squares) are highlighted.

amount of proteins involved in assimilatory sulfate reduction decreased in the presence of reduced sulfur compounds, as exemplified for CysP, a subunit of the sulfate transporter CysAWTP, and CysN, the large subunit of assimilatory ATP sulfurylase (43).

We also compared 2D gels for *A. vinosum* cells exposed to different reduced sulfur compounds for only 8 h (sulfide and thiosulfate) or 24 h (elemental sulfur) with gels obtained for cells that had been grown for a second round on fresh medium supplemented with the respective sulfur sources. Significant differences in collective proteins were not observed, proving that the organism's adaptation of protein composition to the altered environment was already complete after the first period of exposition.

Proteomic profiling using tandem mass tags. As a complementary approach, global proteomic profiling via tandem mass tag experiments was performed. *A. vinosum* cultures were grown under exactly the same conditions as described for comparative 2D gel electrophoresis. For each culture, the soluble and membrane protein fractions were prepared and quantified using tandem mass tags. A total of 1,877 proteins were detected by at least two peptides; 1,848 of these were quantified (see Table S2 in the supplemental material). It should be noted that the first centrifugation step performed immediately after cell disruption by sonication not only removes cell debris. When present, sulfur globules are also sedimented due to their high density (44). We therefore also specifically analyzed the proteins associated with these globules and indeed identified 78 additional proteins that occur exclusively in the sulfur globule proteome, increasing the total number to 1,955 of the 3,302 proteins predicted by the *A. vinosum* genome sequence (59.2%).

We then reasoned, that the most abundant proteins under all growth conditions should represent the basic equipment of an actively growing prokaryotic cell (e.g., ribosomes and chaperones) and should also contain constitutive enzymes catalyzing metabolic pathways of major importance for survival of a purple sulfur bacterium. Indeed, the proteins that overlapped among the 150 most abundant for each of the conditions contained 39 ribosomal or ribosome-associated proteins (including EF-TU) and several chaperonins, as well as seven subunits of F_0F_1 ATP synthase and

adenylate kinase. As expected for a phototrophic organism growing in the light, antenna complex and reaction center subunits were also among the most frequently detected proteins under all conditions (see Table S2 in the supplemental material). Furthermore, the cells always contained large amounts of enzymes involved in central carbon metabolic pathways, i.e., carbon dioxide fixation (RbcAB, fructose-bisphosphate aldolase, and ribulose-phosphate epimerase), gluconeogenesis, and anaplerotic reactions, including enzymes of the glyoxylate cycle (e.g., pyruvate carboxylase, isocitrate lyase, and malic enzyme). Notably, both subunits of flavocytochrome *c* sulfide dehydrogenase, SoxL, SoxYZ, and TusA were also found in the common set of very abundant proteins (see Table S2). FccB, TusA, and SoxL also rendered conspicuous spots upon 2D PAGE (Fig. 1). In addition, we detected great quantities of the cytoplasmically located glutathione amide reductase subunit GarA, lending indirect support to the idea that its substrate glutathione (amide) may be of central importance for transport of sulfur between different cellular compartments (2).

In the next step, we analyzed the proteome data sets acquired via tandem mass spectrometry for significant changes between growth conditions. We considered a protein to be regulated when its level changed at least 1.5-fold. Applying this threshold, relative levels of 151, 93, and 93 proteins increased with growth on sulfide, thiosulfate, and elemental sulfur, respectively, compared to levels for growth on malate (see Fig. S3 and Table S2 in the supplemental material). On the other hand, relative levels of 113, 49, and 70 proteins decreased significantly with growth on sulfide, thiosulfate, and elemental sulfur, respectively (see Fig. S3 and Table S2). Where available, changes observed via comparative 2D gel electrophoresis corresponded to those resulting from the mass tag approach, thereby confirming the latter (see Table S2).

A significant number of changes observed on the proteome level paralleled those on the transcriptome level (13), albeit the factor of increase or decrease was generally much bigger for the changes in relative mRNA levels. Here, we will not attempt to give an overview of all changes observed. Rather, we use the data sets generated in the course of the current study for identification of

TABLE 1 Proteins for which levels of relative abundance rose by at least 1.5-fold with growth on two of the sulfur compounds studied and for which relative mRNA levels (13) increased a minimum of 2-fold under at least one of these conditions^a

Locus tag	Name	Annotation	Avg fold change with growth on:		
			Sulfide	Thiosulfate	Sulfur
Alvin_0492		Hypothetical protein Alvin_0492	0.8	1.2	2.2
Alvin_0680		Protein of unknown function DUF1271	1.4	2.6	2.9
Alvin_1172		Pyruvate flavodoxin/ferredoxin oxidoreductase domain protein	1.6	1.4	1.8
Alvin_1295	SulP	Sulfate transporter	1.9	1.8	2.2
Alvin_1317	SreA	Molybdopterin oxidoreductase Fe4S4 region	2.0	0.9	1.2
Alvin_1323	GarB	Glutathione-disulfide reductase	1.2	1.5	1.6
Alvin_1324	GarA	Redoxin domain protein	1.2	1.7	1.6
Alvin_1365	RbcA	Ribulose-bisphosphate carboxylase	2.3	1.0	1.3
Alvin_1366	RbcB	Ribulose-bisphosphate carboxylase	2.2	1.1	1.1
Alvin_1394		Cytochrome <i>b</i> ₅₆₁	4.7	1.9	2.4
Alvin_1502		PilT domain-containing protein	2.3	1.3	1.0
Alvin_1503	GlgP	Glycogen/starch/alpha-glucan phosphorylase	1.7	1.5	1.6
Alvin_1508		Sulfur relay protein, TusE/DsrC/DsvC family	1.8	1.7	1.9
Alvin_1848	AceA	Isocitrate lyase	0.5	2.0	1.9
Alvin_1971		Coproporphyrinogen dehydrogenase	1.1	1.7	1.9
Alvin_2001		Putative transcriptional regulator, Crp/Fnr family	3.2	1.8	3.2
Alvin_2107		Hypothetical protein Alvin_2107	0.4	1.9	1.5
Alvin_2019		Carbonic anhydrase	2.3	3.2	4.2
Alvin_2037	Isp2	DsrK-like protein	3.2	1.8	2.6
Alvin_2038	Isp1	DsrM-like protein	3.0	2.0	1.7
Alvin_2136		Hypothetical protein Alvin_2136	3.4	1.0	1.2
Alvin_2421	NuoJ	NADH-ubiquinone/plastoquinone oxidoreductase chain 6	1.9	1.7	1.6
Alvin_2577		Antenna complex alpha/beta subunit	3.5	1.1	3.1
Alvin_2705		Hemerythrin-like metal-binding protein	2.3	2.4	2.4
Alvin_2965		TPR repeat-containing protein	0.9	1.6	2.7
Alvin_3032		Hypothetical protein Alvin_3032	3.3	2.5	4.5
Alvin_3052	GltA	Citrate synthase I	2.1	1.7	1.3

^a Bold type indicates cases where relative protein and mRNA levels both exceeded the threshold. During growth with sulfur compounds as electron donors, the only carbon source is CO₂. Proteins known to be involved in dissimilatory sulfur metabolism are excluded here and are compiled in Table 3.

further proteins that are especially important or even vital for sustaining growth under photolithoautotrophic conditions on sulfur compounds. To this end, we applied very strict criteria and compiled lists of proteins that exhibited especially strong changes on the proteome level, as well as significant changes of the respective relative mRNA levels. In Table 1, those cases in which the protein level rose minimally 1.5-fold with growth on at least two of the sulfur compounds tested and the mRNA level rose minimally 2-fold under the same condition are listed. In Table 2, the same criteria were applied, but only significant decreases in protein and mRNA levels were considered. This approach allowed us to draw some general conclusions that will be briefly described before we turn in more detail to conspicuous changes that are or could be specifically related to dissimilatory sulfur oxidation.

General responses. *A. vinosum* cells grown in the absence of malate with CO₂ as the sole carbon source exhibited elevated relative protein levels for components of the carbon dioxide fixation machinery, i.e., carbonic anhydrase Alvin_2019 and the major RuBisCO species RbcAB (Table 1), matching previous results (45). In this work, we found a second carbonic anhydrase, Alvin_0243, to be 10 times more abundant than Alvin_2019 but not affected by the change in carbon source (see Table S2 in the supplemental material). This suggests that Alvin_0243 is the major and constitutive carbonic anhydrase in *A. vinosum*, while Alvin_2019 is an inducible form of carbonic anhydrase. RbcSL (Alvin_2749/Alvin_2750), the second RuBisCO species encoded in the genome, was not detected at the protein level and appears to

play only a minor role, in accordance with earlier reports (46). Neither the relative mRNA level nor the protein level for NADP-dependent malic enzyme was affected by the switch from heterotrophic growth on malate to autotrophic growth on carbon dioxide, indicating that this enzyme also exerts an important if not essential role in the absence of external malate. We propose that under autotrophic conditions, malic enzyme acts in the reverse direction, i.e., catalyzes the NADPH₂-dependent reductive carboxylation of pyruvate to malate. In agreement, *Roseobacter denitrificans* has been reported to use malic enzyme mainly to fix 10 to 15% of protein carbon from CO₂ via anaplerotic pathways (47). We further consider it noteworthy that both relative transcript and protein levels for isocitrate lyase (Alvin_1848), the key enzyme of the glyoxylate cycle in *A. vinosum* (48), significantly increased in the presence of elemental sulfur, while they decreased on sulfide (Tables 1 and 2). The glyoxylate cycle as a whole has a bypass function that prevents loss of carbon dioxide and production of NAD[P]H₂ otherwise occurring through the isocitrate dehydrogenase and 2-oxoglutarate dehydrogenase reactions of the tricarboxylic acid (TCA) cycle (49). This bypass function appears to be especially important during growth on elemental sulfur, while the cells appear to minimize this possibility in the presence of sulfide. In anoxygenic anaerobic phototrophs like *A. vinosum*, photosynthesis generates reducing equivalents through light-induced electron transport. Both avoiding an accumulation of reducing equivalents and channeling excess reducing equivalents into autotrophic CO₂ fixation are very important because respi-

TABLE 2 Proteins for which levels of relative abundance decreased by at least 1.5-fold on two of the sulfur compounds studied and for which relative mRNA levels (13) decreased a minimum of 2-fold under at least one condition^a

Locus tag	Name	Annotation	Avg fold change with growth on:		
			Sulfide	Thiosulfate	Sulfur
Alvin_0082	MsrA	Peptide methionine sulfoxide reductase	0.5	1.0	1.2
Alvin_0345		Sulfur relay protein, TusE/DsrC/DsvC family	0.2	0.7	0.6
Alvin_0809		Oxidoreductase FAD/NAD(P)-binding domain protein	0.8	0.5	0.5
Alvin_1102	CsrA	Carbon storage regulator, CsrA	0.6	0.7	0.7
Alvin_1420		Transcriptional regulator, BadM/Rrf2 family	0.1	0.3	0.4
Alvin_1848	AceA	Isocitrate lyase	0.5	2.0	1.9
Alvin_1890	AcqP	Acyl carrier protein	0.3	0.7	0.7
Alvin_2032		Peroxiredoxin	0.4	0.6	1.1
Alvin_2033		Oxidoreductase FAD/NAD(P)-binding domain protein	0.5	0.7	0.7
Alvin_2093		Protein of unknown function DUF2189, transmembrane	0.5	0.8	0.6
Alvin_2247		Cupin 2 conserved barrel domain protein	0.4	0.8	0.7
Alvin_2327	GlnK	Nitrogen regulatory protein P-II	0.4	1.2	0.8
Alvin_2441	CysA	Sulfate ABC transporter, ATPase subunit	0.5	0.6	0.4
Alvin_2448	CysD	Sulfate adenylyltransferase, small subunit	0.5	0.7	0.6
Alvin_2449	CysN	Sulfate adenylyltransferase, large subunit	0.6	0.6	0.5
Alvin_2484	RimM	16S rRNA processing protein RimM	0.7	0.6	0.5
Alvin_2552	PufM	Photosynthetic reaction center, M subunit	0.7	0.7	0.7
Alvin_2662		Peptidase S16 lon domain protein	0.5	0.6	0.7
Alvin_2664		Hypothetical protein Alvin_2664	0.2	1.6	0.8
Alvin_2667	SufA	Iron-sulfur cluster assembly accessory protein	0.5	0.5	0.4
Alvin_2758	PcnB	Poly(A) polymerase	0.3	0.8	0.6
Alvin_2879		Cytochrome <i>c</i> class I	0.4	0.6	0.7
Alvin_3050	RpmE	Ribosomal protein L31	0.5	0.5	0.6

^a Bold type indicates cases where relative protein and mRNA levels both exceeded the threshold. During growth on sulfur compounds as electron donors, the only carbon source is CO₂. Proteins known to be involved in dissimilatory sulfur metabolism are excluded here and are compiled in Table 3.

ration is not possible. Sulfide is a more powerful reductant than elemental sulfur, and thus, consuming excess reducing equivalents produced by photosynthesis is more important in the presence of sulfide. We propose that the gate into the glyoxylate cycle is narrowed in the presence of sulfide, resulting in loss of carbon previously fixed through the TCA cycle, thereby enabling the cells to reoxidize excess reducing equivalents by CO₂ reduction.

Regulation of central carbon metabolism in *A. vinosum* appears to involve the posttranscriptional carbon storage regulator CsrA. Its amount decreases in the absence of malate (Table 2 and Fig. 1). CsrA is a sequence-specific RNA-binding protein that alters translation and/or stability of its mRNA targets (50, 51). The Csr system is assumed to be a master switch between glycolytic and gluconeogenic metabolisms in *E. coli*. It is known that *E. coli* CsrA negatively controls gluconeogenic activities, like those of fructose-1,6-bisphosphatase, phosphoenolpyruvate synthase, and phosphoenolpyruvate carboxykinase (50, 52). Analogously, a reduced CsrA amount could allow more efficient gluconeogenesis under autotrophic conditions in *A. vinosum*.

Assimilatory sulfate reduction is needed for the synthesis of sulfur-containing cell constituents in the absence of reduced sulfur compounds (43). In accordance with the transcriptome data, several central enzymes of this pathway, including the sulfate-activating *cysDN*-encoded ATP sulfurylase, decreased in amount when reduced sulfur compounds were readily available (Table 2 and Fig. 2; also Fig. 1).

Response of established and probable sulfur-oxidizing proteins. The results for those enzymes for which an involvement in oxidative sulfur metabolism has already been proven are compiled in Table 3 and are combined with the data obtained from tran-

scriptome analysis (13) in Fig. 3. From Fig. 3, it is immediately apparent that the conclusions reached by different experimental approaches were similar. The periplasmic sulfide- and thiosulfate-oxidizing enzymes appear to be largely constitutively synthesized, which is in absolute agreement with the longstanding observation that both substrates are instantly oxidized without any lag phase (see also Fig. S1 in the supplemental material). Polysulfides are well-documented intermediates during the formation of sulfur globules from sulfide in *A. vinosum* (16). Significantly increased relative mRNA levels for the genes Alvin_1317-Alvin_1319, encoding the three subunits of a putative sulfur or polysulfide reductase with highest similarities to archaeal SreABC (55), led us to propose that the purple sulfur bacterial protein may be involved in the transformation of polysulfides to stored sulfur (13). A similar function was proposed for the related proteins from *Chlorobaculum tepidum* (56) and is further supported by the elevated protein levels for Alvin_1317, Alvin_1318, and Alvin_1319 detected during sulfide oxidation (Tables 1 and 3).

As shown in Fig. 3, a low-molecular-weight thiol, possibly glutathione (amide), is proposed to be a carrier molecule transporting sulfur from the periplasmic sulfur globules to the cytoplasmic sulfite-forming machinery. In this context, we noted not only that the protein GarA (Alvin_1324) is highly abundant in *A. vinosum* (see Table S2 in the supplemental material) but that protein levels for GarA and also GarB (Alvin_1323) are significantly higher in the presence of elemental sulfur and thiosulfate than during growth on malate (Table 1). GarA from purple bacteria is a peroxiredoxin/glutaredoxin hybrid that exhibits glutathione amide-dependent peroxidase activity. GarB functions as a glutathione amide reductase (57). Both proteins are predicted to reside in the

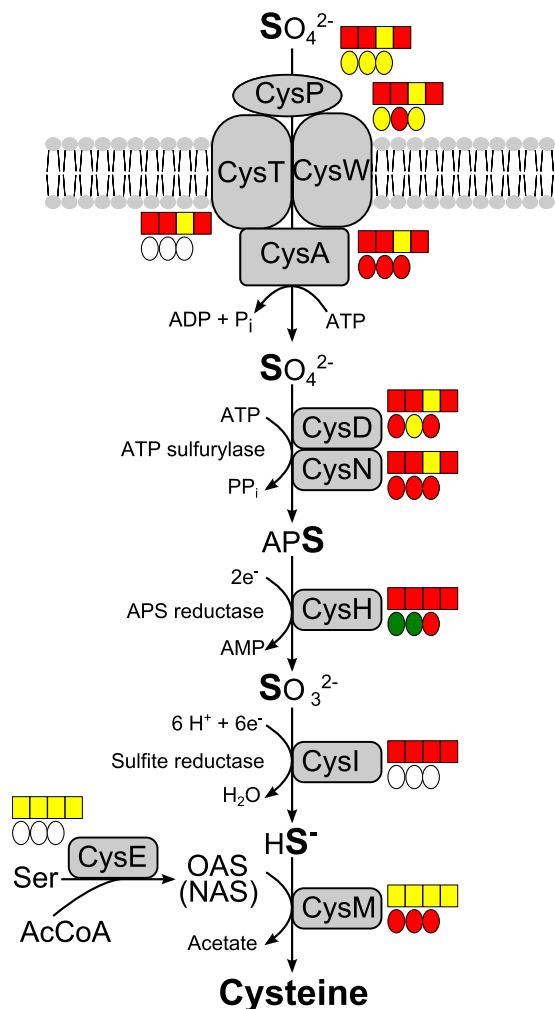


FIG 2 Pathway of assimilatory sulfate reduction in *Allochromatium vinosum*. The proteomic profiles (circles) and transcriptomic profiles (boxes) are depicted next to the respective proteins. Relative fold changes in mRNA levels above 2 (green) were considered significant enhancement. Relative changes smaller than 0.5 (red) were considered to indicate significant decreases in mRNA levels. Relative fold changes between 0.5 and 2 (yellow) indicated unchanged mRNA levels. The same color coding is applied to changes at the protein level. Here, values above 1.5 (green) and below 0.67 (red) were considered significant. Those cases where transcriptomic data were not available or the respective protein was not detected in the proteomic approach are indicated by white squares or circles. Sulfur compounds added, from left to right, are sulfide, thiosulfate, elemental sulfur, and sulfite. Changes on sulfite were not determined on the proteome level. APS, adenosine-5'-phosphosulfate; OAS, O-acetylserine; NAS, N-acetylserine.

cytoplasm in *A. vinosum*. Possible glutathione transporters encoded by Alvin_0481-Alvin_0482 and Alvin_1430-Alvin_1433 were detected in the proteome; however, neither changes in their abundance nor changes in the corresponding relative mRNA levels were observed.

Recently, we established the rhodanese-like protein Alvin_2599, *A. vinosum* TusA (Alvin_2600), and possibly also the membrane-bound DsrE2 protein (Alvin_2601) as components of a cytoplasmic sulfur relay system that, once the carrier persulfide arrives in the cytoplasm, transfers the sulfane sulfur via DsrEFH to the substrate-donating protein of the Dsr pathway, DsrC (19;

Stockdreher et al., submitted). In support of these findings and also in complete agreement with transcriptomic data (13), specifically elevated protein amounts were detected for each of these proteins in our tandem mass tag experiments on at least one of the tested sulfur sources (Fig. 3 and Table 3). We also detected further probable rhodanese-like sulfurtransferases, namely, Alvin_0258, Alvin_0866, and Alvin_3028, in the *A. vinosum* proteome. None of these showed noteworthy changes in amounts of corresponding protein during growth on sulfur compounds (see Table S2 in the supplemental material). Alvin_0866 is highly abundant (see Table S2), and its close genomic linkage with chaperone HscB may indicate an involvement in biosynthesis of [FeS] clusters (58; Stockdreher et al., submitted).

Very distinctive changes were detected for the proteins of the Dsr pathway, especially for DsrAB, DsrE, DsrF, and DsrL, with up to 12-fold increases in cells grown on reduced sulfur compounds (Table 3 and Fig. 3), emphasizing the central importance of this pathway (17, 18, 35, 59). Corresponding to the findings of our transcriptome study (13), increases in relative protein amounts for DsrC were less pronounced than those for DsrAB, DsrEF, and DsrL (Table 3). The *dsrC* gene is constitutively transcribed from an additional, separate promoter site, and the respective transcript amounts under photoheterotrophic conditions were found to be much higher than those for the other studied *dsr* genes (60). In agreement, we identified DsrC as the most abundant Dsr protein during photoorganoheterotrophic growth on malate (see Table S2 in the supplemental material). In addition to DsrC, the genome of *A. vinosum* encodes four more TusE/DsrC/DsvC family sulfur relay proteins (6): Alvin_0345 contains both, Alvin_0732 one, and the other DsrC homologs none of the conserved cysteine residues. Except for Alvin_0028, all DsrC homologs were detected in the proteome. The amount of Alvin_0345 decreased (Table 2), while that of Alvin_1508 increased significantly, on all sulfur compounds (Table 1). There is currently no experimental evidence that would allow assigning functions to these proteins. For the cysteineless Alvin_1508 protein, a role in sulfur transfer is very unlikely. Its function may lie in transcriptional regulation. We have shown before that the DsrC protein encoded in the *A. vinosum* *dsr* gene cluster not only contains a helix-turn-helix motif but also is capable of binding to the DNA region immediately upstream of *dsrA* (60).

An increase in the amounts of the cytoplasmic sulfite-oxidizing enzymes was evident on sulfide (~1.5-fold) (Table 3, Fig. 3). Sulfate, the final product of sulfur oxidation in *A. vinosum*, is formed in the cytoplasm and needs to be exported. One probable transporter involved in this process (SulP; Alvin_1295) exhibited elevated protein and mRNA levels (Table 1).

Of the proteins Alvin_1468, Alvin_1196/1197, Alvin_2093, and Alvin_3072, for which a participation in dissimilatory sulfur metabolism was demonstrated previously by a reverse-genetics approach (13), Alvin_1468 and Alvin_2093 were detected in the *A. vinosum* proteome (see Table S2 in the supplemental material). Alvin_1468 appears to be especially highly abundant (see Table S2). Alvin_1196, Alvin_1197, and Alvin_3072 probably escaped detection because all three are very small transmembrane proteins (32, 32 and 61 amino acids [aa], respectively) (13).

We have previously pointed out a significant increase in mRNA levels on sulfide for the *A. vinosum* gene cluster Alvin_2036-Alvin_2040, encoding a so-called Isp hydrogenase (13, 61–63). The two genes encoding the periplasmically located large

TABLE 3 Different relative protein levels for *A. vinosum* proteins with established functions in oxidative sulfur metabolism^a

Locus tag	Name	Annotation	Avg fold change for growth on:			Reference(s)
			Sulfide	Thiosulfate	Sulfur	
Alvin_0091	TsdA	Thiosulfate dehydrogenase	— ^b	—	—	7
Alvin_0358	SgpB	Sulfur globule protein	S ^c	S	S	15
Alvin_1092	FccB	Flavocytochrome <i>c</i> sulfide dehydrogenase flavin-binding protein	1.0	1.1	1.2	10
Alvin_1093	FccA	Cytochrome <i>c</i> class I	1.0	1.1	1.2	10
Alvin_1118	Sat	Sulfate adenylyltransferase	1.6	1.0	1.2	53
Alvin_1119	AprM	Hypothetical protein Alvin_1119	0.5	0.5	0.7	53
Alvin_1120	AprB	Adenylylsulfate reductase, beta subunit	1.4	0.8	1.1	54
Alvin_1121	AprA	Adenylylsulfate reductase, alpha subunit	1.4	0.9	1.1	54
Alvin_1195	SqrF	FAD-dependent pyridine nucleotide-disulfide oxidoreductase	0.9	0.9	1.0	11
Alvin_1251	DsrA	DsrA	4.2	3.7	5.3	17
Alvin_1252	DsrB	DsrB	10.2	4.5	11.8	17
Alvin_1253	DsrE	DsrE	4.0	2.7	2.1	17
Alvin_1254	DsrF	DsrF	5.0	2.6	2.8	17
Alvin_1255	DsrH	DsrH	S	S	S	17
Alvin_1256	DsrC	DsrC	2.1	1.3	2.5	17
Alvin_1257	DsrM	DsrM	2.6	1.9	1.7	17
Alvin_1258	DsrK	DsrK	2.7	1.8	2.1	17
Alvin_1259	DsrL	DsrL	4.0	4.1	4.7	18
Alvin_1260	DsrJ	DsrJ	2.4	1.6	2.3	18
Alvin_1261	DsrO	DsrO	2.3	1.5	1.6	18
Alvin_1262	DsrP	DsrP	—	—	—	18
Alvin_1263	DsrN	DsrN	—	—	—	18
Alvin_1264	DsrR	DsrR	1.3	1.1	1.2	18
Alvin_1265	DsrS	DsrS	—	—	—	18
Alvin_1317	SreA	Molybdopterin oxidoreductase 4Fe-4S region, cytoplasm	2.0	0.9	1.2	55
Alvin_1318	SreB	4Fe-4S ferredoxin iron-sulfur-binding domain protein	1.7	0.8	1.2	55
Alvin_1319	SreC	Polysulfide reductase NrfD	2.1	1.1	1.4	55
Alvin_1325	SgpC	Sulfur globule protein SgpC	S	S	S	15
Alvin_1905	SgpA	Sulfur globule protein SgpA	S	S	S	15
Alvin_2111	SoxY	SoxY	1.2	1.1	1.2	9
Alvin_2112	SoxZ	SoxZ	1.0	1.2	1.3	9
Alvin_2145	SqrD	Sulfide-quinone reductase	1.6	1.1	1.0	
Alvin_2167	SoxB	SoxB	1.1	1.2	1.2	9
Alvin_2168	SoxX	SoxX	0.7	1.4	1.0	9
Alvin_2169	SoxA	SoxA	1.0	1.3	1.3	9
Alvin_2170	SoxK	SoxXA-binding protein	1.0	1.4	1.2	9
Alvin_2171	SoxL	Sulfur transferase, periplasm	1.3	1.2	1.1	9, 12
Alvin_2489	SoeA	DMSO reductase anchor subunit (DmsC)	1.5	1.1	1.2	22
Alvin_2490	SoeB	4Fe-4S ferredoxin iron-sulfur binding domain protein	1.3	1.1	1.2	22
Alvin_2491	SoeC	Molybdopterin oxidoreductase	1.3	1.0	1.2	22
Alvin_2599	Rhd_2599	Rhodanese domain-containing protein	1.6	1.1	1.2	Stockdreher et al., submitted
Alvin_2600	TusA	TusA	0.8	1.6	1.4	Stockdreher et al., submitted
Alvin_2601	DsrE2	DsrE2	1.3	1.3	1.5	Stockdreher et al., submitted

^a Changes of ≥ 1.5 -fold are highlighted in bold.^b —, not detected.^c S, detected in S-globule proteome.

and small hydrogenase subunits embrace two additional open reading frames, called *isp1* and *isp2*. *Isp1* belongs to the same cytochrome *b* superfamily as DsrM, and *Isp2* has high sequence similarity to DsrK and the catalytic HdrD subunit of heterodisulfide reductases from *Methanosarcina barkeri* (62), pointing to a possible connection to sulfur metabolism. In our current study, we detected and quantified the large subunit of the hydrogenase, as well as the DsrM-like and DsrK-like proteins (see Table S2 in the supplemental material). Notably, the amounts of *Isp1* and

Isp2 increased significantly on all tested sulfur compounds (Table 1), yielding further support to the idea that hydrogen and sulfur metabolism in purple sulfur bacteria are intimately intertwined (13, 63) and identifying the Alvin_2036-Alvin_2040 locus as an important target for reverse genetics.

One further protein with a probable direct connection to oxidative sulfur metabolism showed a very significant positive response in abundance on the protein as well as the mRNA levels (Table 1): Alvin_1394 is a *b*-type cytochrome encoded immedi-

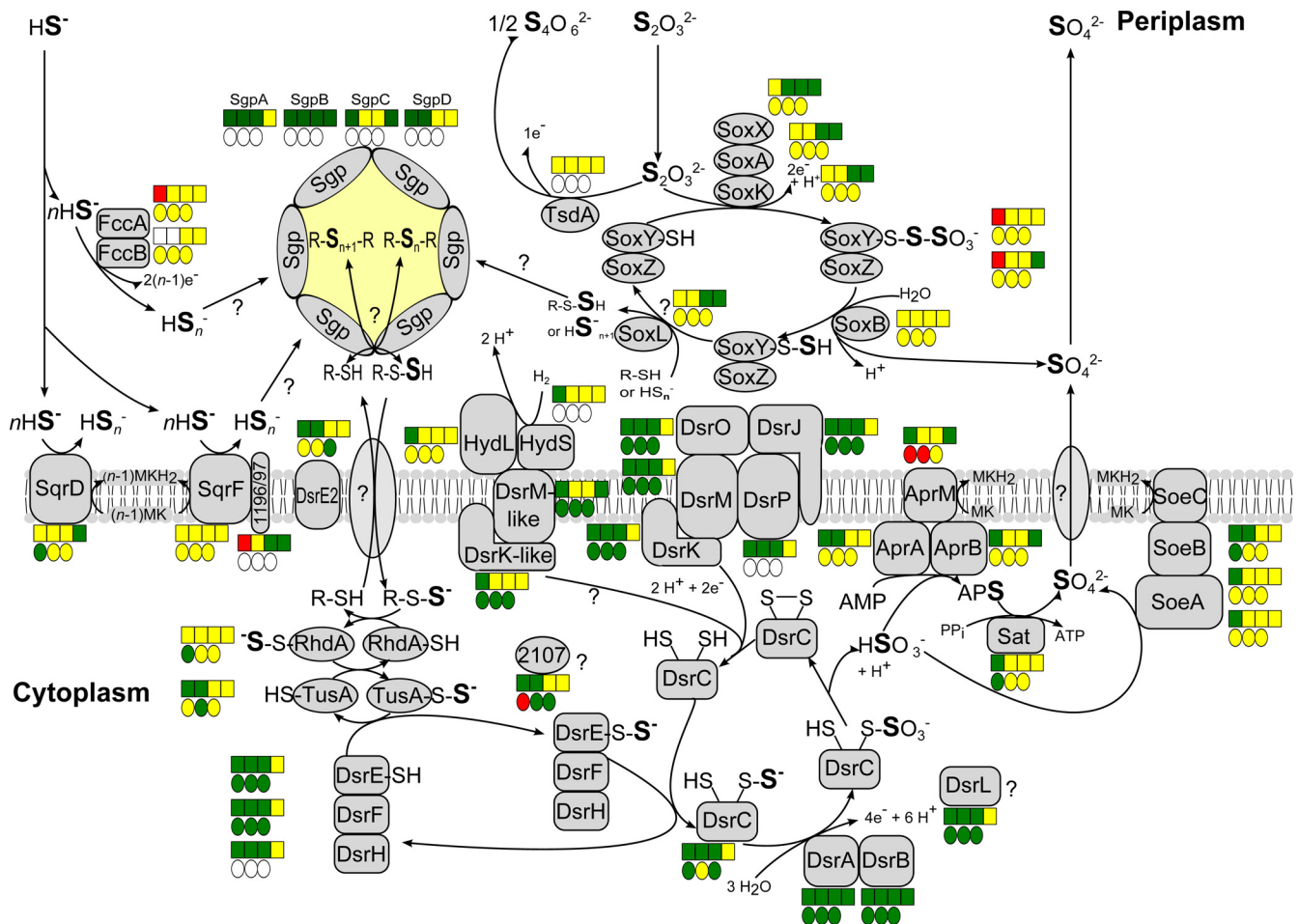


FIG 3 Current model of sulfur oxidation in *Allochromatium vinosum*. The proteomic profiles (circles) and transcriptomic profiles (boxes) are depicted next to the respective proteins. Relative fold changes in mRNA levels above 2 (green) were considered significant enhancement. Relative changes smaller than 0.5 (red) were considered to indicate significant decreases in mRNA levels. Relative fold changes between 0.5 and 2 (yellow) indicated unchanged mRNA levels. The same color coding is applied to changes on the protein level. Here, values above 1.5 (green) and below 0.67 (red) were considered significant. Those cases where transcriptomic data were not available or the respective protein was not detected in the proteomic approach are indicated by white squares or circles. Sulfur compounds added, from left to right, are sulfide, thiosulfate, elemental sulfur, and sulfite. Changes on sulfite were not determined on the proteome level.

ately next to a gene for a probable octaheme tetrathionate reductase (Alvin_1395). The latter also showed a high increase in its relative mRNA level in sulfide-exposed cells (13).

Strongly affected proteins with unknown function. With regard to proteins of unknown function with increased levels observed in the proteomic as well as the transcriptomic approach and encoded in a genetic context indicating a role in oxidative sulfur metabolism, we would like to point out Alvin_2107 (Table 1; see also Fig. S4 in the supplemental material). The gene is situated immediately upstream of and transcribed in the opposite direction from a gene cluster that includes *soxYZ*, encoding the substrate-binding protein of the periplasmic thiosulfate-oxidizing Sox complex (9). Other proteins with strongly positively affected protein and relative mRNA levels in the presence of reduced sulfur compounds include Alvin_3032 (Table 1). Related proteins are restricted to the families *Chromatiaceae*, *Ectothiorhodospiraceae*, *Thioalkalivibrio sulfidophilus* HL-EbGR7, the gene clusters with a gene encoding the DsrC homolog Alvin_1508 and with Alvin_1250, which is situated immediately upstream of *dsrA* in *A. vinosum*.

Among the remaining proteins listed in Table 1, Alvin_0680 exhibits features that point to a possible role in sulfur metabolism. The protein contains an amino-terminal domain of unknown function with three conserved cysteine residues (DUF1271; pfam06902) and two CDGSH-type zinc finger domains that are predicted to bind iron rather than zinc as a redox active pH-labile $[\text{Fe}_2\text{S}_2]$ cluster (64). We would also like to mention Alvin_0232, a probable outer membrane adhesin. Its abundance is significantly higher on elemental sulfur but not on sulfide and thiosulfate, and we therefore consider it a candidate for providing the necessary contact between the water-insoluble elemental sulfur and the bacterial cells (26).

Importance of Isp hydrogenase for sulfur oxidation in *A. vinosum*. The positive response of Isp hydrogenase toward reduced sulfur compounds on the transcriptional and protein levels prompted us to replace the complete Alvin_2036-Alvin_2040 gene cluster between the ATG start codon of Alvin_2040 and the TAG stop codon of Alvin_2036 with a Ω kanamycin interposon and to study the effect of Isp hydrogenase deficiency on oxidative sulfur metabolism in *A. vinosum*. Downstream effects of the inter-

TABLE 4 Phenotypic analysis of *A. vinosum* wild type and $\Delta 2036-2040::\Omega$ Km and $\Delta 2107::\Omega$ Km mutant strains^a

A. vinosum genotype	Value for growth on:		22 mM malate		8 mM sulfide		4 mM thiosulfate		50 mM S ⁰		5 mM sulfite
	Growth on malate-sulfate medium	t _d on RCV medium (h)	Sulfur formation rate (nmol min ⁻¹ mg ⁻¹)	Sulfate formation rate (nmol min ⁻¹ mg ⁻¹)	Maximum sulfur content (μmol mg ⁻¹)	Thiosulfate oxidation rate (nmol min ⁻¹ mg ⁻¹)	Sulfur formation rate (nmol min ⁻¹ mg ⁻¹)	Maximum sulfur content (μmol mg ⁻¹)	Sulfate formation rate (nmol min ⁻¹ mg ⁻¹)	Sulfate formation rate (nmol min ⁻¹ mg ⁻¹)	Sulfite oxidation rate (nmol min ⁻¹ mg ⁻¹)
WT	+	10.2 ± 0.2	125.3 ± 12.3	169.8 ± 47.0	30.7 ± 1.5	118.0 ± 22.0	43.6 ± 6.5	16.8 ± 0.5	190.8 ± 11.9	59.1 ± 11.8	81.9 ± 5.2
Δ Alvin_2036- Δ Alvin_2040:: Ω Km	+	12.4 ± 0.2	66.1 ± 2.7	149.5 ± 10.4	29.7 ± 0.8	103.8 ± 0.5	33.9 ± 0.6	13.1 ± 0.0	208.1 ± 1.2	73.5 ± 0.9	85.4 ± 6.0
Δ Alvin_2107:: Ω Km	+	9.6 ± 0.3	79.7 ± 3.8	25.1 ± 0.0	28.1 ± 0.0	69.2 ± 0.7	39.6 ± 1.2	24.6 ± 0.4	72.4 ± 5.0	3.9 ± 0.4	90.2 ± 1.6

^a Appreciable amounts of thiosulfate and sulfite were not detected in cultures supplied with 50 mM elemental sulfur. When thiosulfate was added as an electron donor, tetrathionate and sulfite were not detected in the course of the experiments. Experiments were performed in completely filled 250-ml culture bottles at 30°C with saturating light intensity. Values given are means of data for three biological replicates. Initial protein concentrations: 0.03 mg ml⁻¹ for the experiments on malate-sulfate and RCV medium and 0.1 mg ml⁻¹ for the other experiments. Sulfur and sulfate formation rates were calculated for periods of linear increases of sulfur/sulfate concentrations and are given in nmol min⁻¹ per mg protein. Thiosulfate and sulfite oxidation rates were calculated accordingly for periods of linear decreases in thiosulfate/sulfate concentrations. t_d doubling time (hours).

poson can be excluded, because Alvin_2036 represents the last gene of the cluster and the upstream gene Alvin_2035 is transcribed in the opposite direction. The mutant strain did not show any general growth defects or effects on sulfate assimilation, as evidenced by unaltered growth on minimal medium containing malate and sulfate (Table 4). However, the *A. vinosum* Alvin_2036- Δ Alvin_2040:: Ω Km strain showed a strong phenotype when exposed to 8 mM sulfide. The rate of deposition of intracellular sulfur from sulfide was significantly reduced compared to that for the wild type. This effect became even more pronounced with lower initial protein concentrations (not shown). In contrast, the oxidation of thiosulfate (4 mM), elemental sulfur (50 mM), and sulfite (5 mM) was unimpaired (Table 4). These findings clearly support the suggestion that Isp hydrogenase exerts an important function during sulfur oxidation in *A. vinosum* and more precisely locates its role in the transformation of sulfide to intracellularly stored sulfur. Sequence analyses previously led to the proposal that the HydSL (HynSL in *Thiocapsa roseopersicina*)-Isp1-Isp2 complex may be able to transfer electrons stemming from hydrogen oxidation in the periplasm via the membrane-bound DsrM-like *b*-type cytochrome and the membrane-associated, cytoplasmically oriented DsrK-like protein onto a cytoplasmic (hetero)disulfide (63). In Fig. 3, we suggest that the intramolecular DsrC disulfide could be a substrate for Isp hydrogenase and that this reaction could establish the link between hydrogen and sulfur metabolisms. Still, the question remains how the hydrogen needed for such a reaction is generated. Under nitrogen-fixing conditions, the nitrogenase-catalyzed reaction could be a main source, but the experiments described here were performed under nitrogenase-repressing conditions. We consider the possibility that *A. vinosum* reduces protons to hydrogen in the cytoplasm, possibly as a means of disposing of excess reducing power in the presence of high initial sulfide concentrations. *A. vinosum* cells contain a cytoplasmic hydrogenase that could in principle exert such a function: three of the four subunits (HydA, HydG, and HydB, i.e., Alvin_0807, Alvin_0809, and Alvin_0810) of a protein resembling the NADPH₂-dependent sulfhydrogenase from the archaeon *Pyrococcus furiosus* (65, 66) were found in the proteome, and the amount of HydB was elevated 4.5-fold on sulfide. The cytoplasmic reduction of protons with NAD(P)H₂ could be made possible by diffusion of the produced hydrogen over the cytoplasmic membrane, where it could instantly be reoxidized by Isp hydrogenase, thus even generating a proton gradient. While this idea still awaits experimental proof and other electron transfer models can be thought of, it has been independently shown that Isp1 and Isp2 are critical for *in vivo* hydrogen cycling in the purple sulfur bacterium *Thiocapsa roseopersicina* BBS and that HynSL is expressed in the presence of thiosulfate in this organism (62). Furthermore, a direct linkage between hydrogen and sulfur metabolism via Isp (Hyn) hydrogenase was also recognized in *T. roseopersicina*. In the dark, H₂ consumption catalyzed by this hydrogenase is connected to utilization of S⁰ as an electron acceptor and results in the accumulation of H₂S (67).

Importance of Alvin_2107 for sulfur oxidation in *A. vinosum*. The nucleotide sequence between the ATG start and TGA stop codons of Alvin_2107 was completely replaced by a Ω kanamycin interposon. Downstream effects of the interposon insertion can be excluded, because the genes upstream and downstream of Alvin_2107 are transcribed in the opposite direction. Photoorganoheterotrophic growth of the Alvin_2107-deficient mutant

strain on malate-containing medium with sulfate as the sole sulfur source was unaffected, thus excluding general growth defects (Table 4). The *A. vinosum* Alvin_2107:: Ω Km mutant exhibited a very pronounced defect with regard to the oxidation of stored sulfur. While the formation rate of intracellular sulfur from sulfide and the oxidation rate of thiosulfate were only slightly decreased in comparison to those recorded for the wild type, rates for formation of the final product sulfate were drastically reduced in cultures grown with sulfide, thiosulfate, and elemental sulfur. However, when external sulfite was supplied as the substrate, the mutant again behaved just like the wild-type strain (Table 4). Together, these observations clearly narrow the place of action for Alvin_2107 to the processes occurring during the transformation of stored sulfur to sulfite. The slightly decreased rates observed for both the formation of sulfur from sulfide and the oxidation of thiosulfate are most probably an indirect result of the sulfate formation bottleneck. The protein Alvin_2107 is predicted to be localized in the cytoplasm. Notably, the corresponding gene is situated next to *tusA* in some members of the family *Ectothiorhodospiraceae*, i.e., *Halorhodospira halophila* DSM 244 and *Alkalilimnicola ehrlichii* (see Fig. S4C in the supplemental material). Alvin_2107 is present in all genome-sequenced phototrophic members of the *Chromatiaceae* and in the other members of the *Gammaproteobacteria* that use the Dsr pathway of sulfur oxidation. Alvin_2107 is not present in gammaproteobacterial sulfur oxidizers like the acidithiobacilli, which contain the Hdr complex as a probable unit involved in sulfite formation (68). Notably, occurrence of Alvin_2107 is also strictly connected with possession of *dsr* genes in genome-sequenced members of the *Ectothiorhodospiraceae* (see Fig. S4C). In summary, these findings point to a function specifically connected with dissimilatory sulfite reductase and associated proteins. All Alvin_2107 homologous proteins from the *Chromatiaceae* share a conserved cysteine residue, which is, however, not present in proteins occurring outside this family (see Fig. S4B).

Enrichment and subsequent investigation of the sulfur globule proteome. As is evident from the previous discussion, intracellular sulfur globules are eminently important intermediates of reduced sulfur compound oxidation in purple sulfur bacteria like *A. vinosum*. However, the proteins forming the envelope of these globules were not detected in either the soluble or membrane proteome. We therefore enriched sulfur globules and surveyed the proteins associated with them in a separate set of experiments. We thus found 78 previously undetected proteins (see Table S2 in the supplemental material). As a proof of principle, this set contained all the established sulfur globule proteins, SgpA, SgpB, and SgpC (14). SgpC is important for expansion of the globules and was less frequently detected than the other two proteins (see Table S2). The most abundant of the newly identified proteins of the sulfur globule proteome was Alvin_2515, which is encoded in a cluster comprising genes for hydrophobic/amphiphilic exporters and a probable two-component transcriptional regulator (see Fig. S5). Alvin_2515 already attracted attention in the previous transcriptomic study, because its relative mRNA level drastically increased with growth on sulfide and thiosulfate (28-fold/6-fold) (13). Alvin_2515-related genes occur only in genome-sequenced members of the *Chromatiaceae*, all of which produce intracellular sulfur globules. All of the derived proteins are predicted to be synthesized with cleavable-N-terminal signal peptides mediating Sec-dependent transport into the periplasm, just as has been re-

ported for the three established *A. vinosum* sulfur globule proteins (15). Other features shared with SgpA, -B, and -C are a highly repetitive amino acid sequence rich in regularly spaced proline residues and the prediction that Alvin_2515 and its homologs are structural proteins. In fact, coiled-coil segments were determined in Alvin_2515 (see Fig. S5) using the COILS server (69). The coiled coil is a protein motif characterized by superhelical twisting of two or more alpha helices around one another. Coiled-coil proteins can form rod-like tertiary structures and include the intermediate filaments of the metazoan cytoskeleton, as well as bacterium-specific cytoskeletal proteins that typically assemble into stable macromolecular scaffolds (70, 71). Taken together, the exclusive detection in the *A. vinosum* sulfur globule proteome and the properties predicted from the sequence strongly indicate that Alvin_2515 is a new protein of the sulfur globule envelope, which we term SgpD (Fig. 3).

Among the 50 proteins significantly enriched in the sulfur globule proteome, Alvin_1981 and Alvin_2136 appear especially noteworthy, because relative mRNA levels for these were increased 3.6- and 50-fold, respectively, on sulfide (13). Alvin_1981 is a membrane protein and contains a sodium:sulfate symporter domain and some of its homologs are annotated as sulfur deprivation response regulators. Alvin_2136 is a soluble protein. Signal peptide prediction is ambiguous for the *A. vinosum* protein, while the homologous proteins from several other members of the *Chromatiaceae* are predicted to reside in the cytoplasm, i.e., not in the same cellular compartment as the sulfur globules. Finally, we emphasize that none of the established components of the periplasmic sulfide- and thiosulfate-metabolizing enzymes appeared to be enriched with the sulfur globules.

Conclusions. In conclusion, proteomic profiles obtained for the purple sulfur bacterium *A. vinosum* upon exposure to sulfide, thiosulfate, or elemental sulfur compared to findings for photoorganoheterotrophic growth on malate provided global insights into changes in relative protein levels triggered by reduced sulfur compounds. As a whole, the proteome of *A. vinosum* stayed quite stable under the different growth conditions, which can be attributed to the constitutive formation of proteins catalyzing major steps of the dissimilatory sulfur oxidation pathway, i.e., the Sox, Sqr, and Fcc proteins. The data generated during this study confirmed the important roles of established pathways, e.g., the Dsr pathway. The essential Dsr proteins, including reverse-acting sulfite reductase (DsrAB), exhibited the most pronounced changes observed upon exposure of *A. vinosum* to reduced sulfur compounds. Furthermore, Alvin_2107 and the new sulfur globule protein SgpD (Alvin_2515) are obvious examples that show that proteome analysis constitutes an excellent method for the identification of new sulfur metabolism-related genes not only in *A. vinosum* but also in other sulfur-oxidizing bacteria.

ACKNOWLEDGMENTS

This work was supported by the Deutsche Forschungsgemeinschaft (grant Da 351/6-1).

We thank Renate Zigann and Bernhard Gehrig for excellent technical assistance.

REFERENCES

1. Dahl C, Friedrich CG, Kletzin A. 15 December 2008. Sulfur oxidation in prokaryotes. In eLS. John Wiley & Sons, Ltd, Chichester, United Kingdom. <http://dx.doi.org/10.1002/9780470015902.a0021155>.
2. Frigaard N-U, Dahl C. 2009. Sulfur metabolism in phototrophic sulfur

- bacteria. *Adv. Microb. Physiol.* 54:103–200. [http://dx.doi.org/10.1016/S0065-2911\(08\)00002-7](http://dx.doi.org/10.1016/S0065-2911(08)00002-7).
3. Imhoff JF. 2005. Family I. Chromatiaceae Bavendamm 1924, 125^{AL} emend. Imhoff 1984b, 339, p 3–40. In Brenner DJ, Krieg NR, Staley JT, Garrity GM (ed), *Bergey's manual of systematic bacteriology*, vol 2. Springer, New York, NY.
 4. Pattaragulwanit K, Dahl C. 1995. Development of a genetic system for a purple sulfur bacterium: conjugative plasmid transfer in *Chromatium vinosum*. *Arch. Microbiol.* 164:217–222. <http://dx.doi.org/10.1007/BF02529974>.
 5. Dahl C. 1996. Insertional gene inactivation in a phototrophic sulphur bacterium: APS-reductase-deficient mutants of *Chromatium vinosum*. *Microbiology* 142:3363–3372. <http://dx.doi.org/10.1099/13500872-142-12-3363>.
 6. Weissgerber T, Zigann R, Bruce D, Chang Y-J, Detter JC, Han C, Hauser L, Jeffries CD, Land M, Munk AC, Tapia R, Dahl C. 2011. Complete genome sequence of *Allochromatium vinosum* DSM 180^T. *Stand. Genomic Sci.* 5:311–330. <http://dx.doi.org/10.4056/signs.2335270>.
 7. Denkmann K, Grein F, Zigann R, Siemen A, Bergmann J, van Helmont S, Nicolai A, Pereira IAC, Dahl C. 2012. Thiosulfate dehydrogenase: a wide-spread unusual acidophilic c-type cytochrome. *Environ. Microbiol.* 14:2673–2688. <http://dx.doi.org/10.1111/j.1462-2920.2012.02820.x>.
 8. Grein F, Venceslau SS, Schneider L, Hildebrandt P, Todorovic S, Pereira IAC, Dahl C. 2010. DsrJ, an essential part of the DsrMKJOP complex in the purple sulfur bacterium *Allochromatium vinosum*, is an unusual triheme cytochrome c. *Biochemistry* 49:8290–8299. <http://dx.doi.org/10.1021/bi1007673>.
 9. Hensen D, Sperling D, Trüper HG, Brune DC, Dahl C. 2006. Thiosulfate oxidation in the phototrophic sulphur bacterium *Allochromatium vinosum*. *Mol. Microbiol.* 62:794–810. <http://dx.doi.org/10.1111/j.1365-2958.2006.05408.x>.
 10. Reinartz M, Tschäpe J, Brüser T, Trüper HG, Dahl C. 1998. Sulfide oxidation in the phototrophic sulfur bacterium *Chromatium vinosum*. *Arch. Microbiol.* 170:59–68. <http://dx.doi.org/10.1007/s002030050615>.
 11. Gregersen LH, Bryant DA, Frigaard N-U. 2011. Mechanisms and evolution of oxidative sulfur metabolism in green sulfur bacteria. *Front. Microbiol.* 2:116. <http://dx.doi.org/10.3389/fmicb.2011.00116>.
 12. Welte C, Hafner S, Krätzer C, Quentmeier AT, Friedrich CG, Dahl C. 2009. Interaction between Sox proteins of two physiologically distinct bacteria and a new protein involved in thiosulfate oxidation. *FEBS Lett.* 583:1281–1286. <http://dx.doi.org/10.1016/j.febslet.2009.03.020>.
 13. Weissgerber T, Dobler N, Polen T, Latus J, Stockdreher Y, Dahl C. 2013. Genome-wide transcriptional profiling of the purple sulfur bacterium *Allochromatium vinosum* DSM 180^T during growth on different reduced sulfur compounds. *J. Bacteriol.* 195:4231–4245. <http://dx.doi.org/10.1128/JB.00154-13>.
 14. Brune DC. 1995. Isolation and characterization of sulfur globule proteins from *Chromatium vinosum* and *Thiocapsa roseopersicina*. *Arch. Microbiol.* 163:391–399. <http://dx.doi.org/10.1007/BF00272127>.
 15. Pattaragulwanit K, Brune DC, Trüper HG, Dahl C. 1998. Molecular genetic evidence for extracytoplasmic localization of sulfur globules in *Chromatium vinosum*. *Arch. Microbiol.* 169:434–444. <http://dx.doi.org/10.1007/s002030050594>.
 16. Prange A, Engelhardt H, Trüper HG, Dahl C. 2004. The role of the sulfur globule proteins of *Allochromatium vinosum*: mutagenesis of the sulfur globule protein genes and expression studies by real-time RT PCR. *Arch. Microbiol.* 182:165–174. <http://dx.doi.org/10.1007/s00203-004-0683-3>.
 17. Pott AS, Dahl C. 1998. Sirohaem-sulfite reductase and other proteins encoded in the *dsr* locus of *Chromatium vinosum* are involved in the oxidation of intracellular sulfur. *Microbiology* 144:1881–1894. <http://dx.doi.org/10.1099/00221287-144-7-1881>.
 18. Dahl C, Engels S, Pott-Sperling AS, Schulte A, Sander J, Lübke Y, Deuster O, Brune DC. 2005. Novel genes of the *dsr* gene cluster and evidence for close interaction of Dsr proteins during sulfur oxidation in the phototrophic sulfur bacterium *Allochromatium vinosum*. *J. Bacteriol.* 187:1392–1404. <http://dx.doi.org/10.1128/JB.187.4.1392-1404.2005>.
 19. Stockdreher Y, Venceslau SS, Josten M, Sahl HG, Pereira IAC, Dahl C. 2012. Cytoplasmic sulfurtransferases in the purple sulfur bacterium *Allochromatium vinosum*: evidence for sulfur transfer from DsrEFH to DsrC. *PLoS One* 7:e40785. <http://dx.doi.org/10.1371/journal.pone.0040785>.
 20. Cort JR, Selan UM, Schulte A, Grimm F, Kennedy MA, Dahl C. 2008. *Allochromatium vinosum* DsrC: solution-state NMR structure, redox properties and interaction with DsrEFH, a protein essential for purple sulfur bacterial sulfur oxidation. *J. Mol. Biol.* 382:692–707. <http://dx.doi.org/10.1016/j.jmb.2008.07.022>.
 21. Oliveira TF, Vonnrhein C, Matia PM, Venceslau SS, Pereira IAC, Archer M. 2008. The crystal structure of *Desulfovibrio vulgaris* dissimilatory sulfite reductase bound to DsrC provides novel insights into the mechanism of sulfate respiration. *J. Biol. Chem.* 283:34141–34149. <http://dx.doi.org/10.1074/jbc.M805643200>.
 22. Dahl C, Franz B, Hensen D, Kesselheim A, Zigann R. 2013. Sulfite oxidation in the purple sulfur bacterium *Allochromatium vinosum*: identification of SoeABC as a major player and relevance of SoxYZ in the process. *Microbiology* 159:2626–2638. <http://dx.doi.org/10.1099/mic.0.071019-0>.
 23. Sanchez O, Ferrera I, Dahl C, Mas J. 2001. *In vivo* role of APS reductase in the purple sulfur bacterium *Allochromatium vinosum*. *Arch. Microbiol.* 176:301–305. <http://dx.doi.org/10.1007/s002030100327>.
 24. Jendrossek D. 2009. Polyhydroxyalkanoate granules are complex subcellular organelles (carbonosomes). *J. Bacteriol.* 191:3195–3202. <http://dx.doi.org/10.1128/JB.01723-08>.
 25. Weaver PF, Wall JD, Gest H. 1975. Characterization of *Rhodospseudomonas capsulata*. *Arch. Microbiol.* 105:207–216. <http://dx.doi.org/10.1007/BF00447139>.
 26. Franz B, Lichtenberg H, Hormes J, Modrow H, Dahl C, Prange A. 2007. Utilization of solid “elemental” sulfur by the phototrophic purple sulfur bacterium *Allochromatium vinosum*: a sulfur K-edge XANES spectroscopy study. *Microbiology* 153:1268–1274. <http://dx.doi.org/10.1099/mic.0.2006/003954-0>.
 27. Sambrook J, Fritsch EF, Maniatis T. 1989. *Molecular cloning: a laboratory manual*, 2nd ed. Cold Spring Harbor Laboratory, Cold Spring Harbor, NY.
 28. Horton RM. 1995. PCR mediated recombination and mutagenesis: SOEing together tailor-made genes. *Mol. Biotechnol.* 3:93–99. <http://dx.doi.org/10.1007/BF02789105>.
 29. Simon R, Priefer U, Pühler A. 1983. A broad host range mobilization system for *in vivo* genetic engineering: transposon mutagenesis in gram negative bacteria. *Nat. Biotechnol.* 1:784–791. <http://dx.doi.org/10.1038/nbt1183-784>.
 30. Laemmli UK. 1970. Cleavage of structural proteins during the assembly of the head of bacteriophage T4. *Nature* 227:680–685. <http://dx.doi.org/10.1038/227680a0>.
 31. León IR, Schwämmle V, Jensen NO, Sprenger RR. 2013. Quantitative assessment of in-solution digestion efficiency identifies optimal protocols for unbiased protein analysis. *Mol. Cell. Proteomics* 12:2992–3005. <http://dx.doi.org/10.1074/mcp.M112.025585>.
 32. Manza LL, Stamer SL, Ham AJL, Codreanu SG, Liebler DC. 2005. Sample preparation and digestion for proteomic analyses using spin filters. *Proteomics* 5:1742–1745. <http://dx.doi.org/10.1002/pmic.200401063>.
 33. Masuda T, Tomita M, Ishihama Y. 2008. Phase transfer surfactant-aided trypsin digestion for membrane proteome analysis. *J. Proteome Res.* 7:731–740. <http://dx.doi.org/10.1021/pr700658q>.
 34. Wisniewski JR, Zougman A, Nagaraj N, Mann M. 2009. Universal sample preparation method for proteome analysis. *Nat. Methods* 6:359–362. <http://dx.doi.org/10.1038/nmeth.1322>.
 35. Sander J, Engels-Schwarzlose S, Dahl C. 2006. Importance of the DsrMKJOP complex for sulfur oxidation in *Allochromatium vinosum* and phylogenetic analysis of related complexes in other prokaryotes. *Arch. Microbiol.* 186:357–366. <http://dx.doi.org/10.1007/s00203-006-0156-y>.
 36. Shevchenko A, Tomas H, Havlis J, Olsen JV, Mann M. 2006. In-gel digestion for mass spectrometric characterization of proteins and proteomes. *Nat. Protoc.* 1:2856–2860. <http://dx.doi.org/10.1038/nprot.2006.468>.
 37. Rosenfeld J, Capdevielle J, Guillemot JC, Ferrara P. 1992. In-gel digestion of proteins for internal sequence analysis after 1-dimensional or 2-dimensional gel electrophoresis. *Anal. Biochem.* 203:173–179. [http://dx.doi.org/10.1016/0003-2697\(92\)90061-B](http://dx.doi.org/10.1016/0003-2697(92)90061-B).
 38. Lu P, Vogel C, Wang R, Yao X, Marcotte EM. 2007. Absolute protein expression profiling estimates the relative contributions of transcriptional and translational regulation. *Nat. Biotechnol.* 25:117–124. <http://dx.doi.org/10.1038/nbt1270>.
 39. Pedersen S, Bloch PL, Reeh S, Neidhardt FC. 1978. Patterns of protein synthesis in *Escherichia coli*: a catalog of amount of 140 individual proteins at different growth rates. *Cell* 14:179–190. [http://dx.doi.org/10.1016/0092-8674\(78\)90312-4](http://dx.doi.org/10.1016/0092-8674(78)90312-4).
 40. Verméglio A, Li J, Schoepp-Cothenet B, Pratt N, Knaff DB. 2002. The

- role of high-potential iron protein and cytochrome c_8 as alternative electron donors to the reaction center of *Chromatium vinosum*. *Biochemistry* 41:8868–8875. <http://dx.doi.org/10.1021/bi012037h>.
41. Sahl HG, Trüper HG. 1980. Malic enzyme of *Chromatium vinosum*. *Arch. Microbiol.* 127:17–24. <http://dx.doi.org/10.1007/BF00414350>.
 42. Dahl C, Schulte A, Stockdreher Y, Hong C, Grimm F, Sander J, Kim R, Kim S-H, Shin DH. 2008. Structural and molecular genetic insight into a wide-spread bacterial sulfur oxidation pathway. *J. Mol. Biol.* 384:1287–1300. <http://dx.doi.org/10.1016/j.jmb.2008.10.016>.
 43. Neumann S, Wynen A, Trüper HG, Dahl C. 2000. Characterization of the *cys* gene locus from *Allochromatium vinosum* indicates an unusual sulfate assimilation pathway. *Mol. Biol. Rep.* 27:27–33. <http://dx.doi.org/10.1023/A:1007058421714>.
 44. Guerrero R, Pedros-Alio C, Schmidt TM, Mas J. 1985. A survey of buoyant density of microorganisms in pure cultures and natural samples. *Microbiologia* 1:53–65.
 45. Viale AM, Kobayashi H, Akazawa T. 1990. Distinct properties of *Escherichia coli* products of plant-type ribulose-1,5-bisphosphate carboxylase/oxygenase directed by two sets of genes from the photosynthetic bacterium *Chromatium vinosum*. *J. Biol. Chem.* 265:18386–18392.
 46. Viale AM, Kobayashi H, Akazawa T. 1989. Expressed genes for plant-type ribulose 1,5-bisphosphate carboxylase/oxygenase in the photosynthetic bacterium *Chromatium vinosum*, which possesses two complete sets of genes. *J. Bacteriol.* 171:2391–2400.
 47. Tang KH, Feng XY, Tang YJ, Blankenship RE. 2009. Carbohydrate metabolism and carbon fixation in *Roseobacter denitrificans* OCh114. *PLoS One* 4:e7233. <http://dx.doi.org/10.1371/journal.pone.0007233>.
 48. Fuller RC, Kornberg HL, Sisler EC, Smillie RM. 1961. Carbon metabolism in *Chromatium*. *J. Biol. Chem.* 236:2140–2149.
 49. Kornberg HL. 1959. Aspects of terminal respiration in microorganisms. *Annu. Rev. Microbiol.* 13:49–78. <http://dx.doi.org/10.1146/annurev.mi.13.100159.000405>.
 50. Revelles O, Millard P, Nougayrede JP, Dobrindt U, Oswald E, Letisse F, Portais JC. 2013. The carbon storage regulator (Csr) system exerts a nutrient-specific control over central metabolism in *Escherichia coli* strain Nissle 1917. *PLoS One* 8:e66386. <http://dx.doi.org/10.1371/journal.pone.0066386>.
 51. Romeo T, Vakulskas CA, Babitzke P. 2013. Post-transcriptional regulation on a global scale: form and function of Csr/Rsm systems. *Environ. Microbiol.* 15:313–324. <http://dx.doi.org/10.1111/j.1462-2920.2012.02794.x>.
 52. Timmermans J, Van Melderen L. 2009. Conditional essentiality of the *csrA* gene in *Escherichia coli*. *J. Bacteriol.* 191:1722–1724. <http://dx.doi.org/10.1128/JB.01573-08>.
 53. Parey K, Demmer U, Warkentin E, Wynen A, Ermler U, Dahl C. 2013. Structural, biochemical and genetic characterization of ATP sulfurylase from *Allochromatium vinosum*. *PLoS One* 8:e74707. <http://dx.doi.org/10.1371/journal.pone.0074707>.
 54. Hipp WM, Pott AS, Thum-Schmitz N, Faath I, Dahl C, Trüper HG. 1997. Towards the phylogeny of APS reductases and sirohaem sulfite reductases in sulfate-reducing and sulfur-oxidizing prokaryotes. *Microbiology* 143:2891–2902. <http://dx.doi.org/10.1099/00221287-143-9-2891>.
 55. Laska S, Lottspeich F, Kletzin A. 2003. Membrane-bound hydrogenase and sulfur reductase of the hyperthermophilic and acidophilic archaeon *Acidianus ambivalens*. *Microbiology* 149:2357–2371. <http://dx.doi.org/10.1099/mic.0.26455-0>.
 56. Eddie BJ, Hanson TE. 2013. *Chlorobaculum tepidum* TLS displays a complex transcriptional response to sulfide addition. *J. Bacteriol.* 195:399–408. <http://dx.doi.org/10.1128/JB.01342-12>.
 57. Vergauwen B, Pauwels F, Jacquemotte F, Meyer TE, Cusanovich MA, Bartsch RG, van Beeumen JJ. 2001. Characterization of glutathione amide reductase from *Chromatium gracile*. Identification of a novel thiol peroxidase (Prx/Grx) fueled by glutathione amide redox cycling. *J. Biol. Chem.* 276:20890–20897. <http://dx.doi.org/10.1074/jbc.M102026200>.
 58. Kim JH, Tonelli M, Frederick RO, Chow DC, Markley JL. 2012. Specialized Hsp70 chaperone (HscA) binds preferentially to the disordered form, whereas J-protein (HscB) binds preferentially to the structured form of the iron-sulfur cluster scaffold protein (IscU). *J. Biol. Chem.* 287:31406–31413. <http://dx.doi.org/10.1074/jbc.M112.352617>.
 59. Lübke YJ, Youn H-S, Timkovich R, Dahl C. 2006. Siro(haem)amide in *Allochromatium vinosum* and relevance of DsrL and DsrN, a homolog of cobyrinic acid *a,c* diamide synthase for sulphur oxidation. *FEMS Microbiol. Lett.* 261:194–202. <http://dx.doi.org/10.1111/j.1574-6968.2006.00343.x>.
 60. Grimm F, Dobler N, Dahl C. 2010. Regulation of *dsr* genes encoding proteins responsible for the oxidation of stored sulfur in *Allochromatium vinosum*. *Microbiology* 156:764–773. <http://dx.doi.org/10.1099/mic.0.034645-0>.
 61. Dahl C, Rákhely G, Pott-Sperling AS, Fodor B, Takács M, Tóth A, Kraeling M, Györfi K, Kovács A, Tusz J, Kovács KL. 1999. Genes involved in hydrogen and sulfur metabolism in phototrophic sulfur bacteria. *FEMS Microbiol. Lett.* 180:317–324. <http://dx.doi.org/10.1111/j.1574-6968.1999.tb08812.x>.
 62. Palágyi-Mészáros LS, Maróti J, Latinovics D, Balogh T, Klement E, Medzihradský KF, Rákhely G, Kovács KL. 2009. Electron-transfer subunits of the NiFe hydrogenases in *Thiocapsa roseopersicina* BBS. *FEBS J.* 276:164–174. <http://dx.doi.org/10.1111/j.1742-4658.2008.06770.x>.
 63. Pandelia M-E, Lubitz W, Nitschke W. 2012. Evolution and diversification of group 1 [NiFe] hydrogenases. Is there a phylogenetic marker for O₂-tolerance? *Biochim. Biophys. Acta* 1817:1565–1575. <http://dx.doi.org/10.1016/j.bbabi.2012.04.012>.
 64. Wiley SE, Paddock ML, Abresch EC, Gross L, van der Geer P, Nechushtai R, Murphy AN, Jennings PA, Dixon JE. 2007. The outer mitochondrial membrane protein mitoNEET contains a novel redox-active 2Fe-2S cluster. *J. Biol. Chem.* 282:23745–23749. <http://dx.doi.org/10.1074/jbc.C700107200>.
 65. Pedroni P, della Volpe A, Galli G, Mura GM, Pratesi C, Grandi G. 1995. Characterization of the locus encoding the [NiFe] sulfhydrogenase from the archaeon *Pyrococcus furiosus*: evidence for a relationship to bacterial sulfite reductases. *Microbiology* 141:449–458. <http://dx.doi.org/10.1099/13500872-141-2-449>.
 66. Silva PJ, de Castro B, Hagen WR. 1999. On the prosthetic groups of the NiFe sulfhydrogenase from *Pyrococcus furiosus*: topology, structure, and temperature-dependent redox chemistry. *J. Biol. Inorg. Chem.* 4:284–291. <http://dx.doi.org/10.1007/s007750050314>.
 67. Laurinavichene TV, Rákhely G, Kovács KL, Tsygankov AA. 2007. The effect of sulfur compounds on H₂ evolution/consumption reactions, mediated by various hydrogenases, in the purple sulfur bacterium, *Thiocapsa roseopersicina*. *Arch. Microbiol.* 188:403–410. <http://dx.doi.org/10.1007/s00203-007-0260-7>.
 68. Quatrini R, Appia-Ayme C, Denis Y, Jedlicki E, Holmes DS, Bonnefoy V. 2009. Extending the models for iron and sulfur oxidation in the extreme acidophile *Acidithiobacillus ferrooxidans*. *BMC Genomics* 10:394. <http://dx.doi.org/10.1186/1471-2164-10-394>.
 69. Lupas A, Vandyke M, Stock J. 1991. Predicting coiled coils from protein sequences. *Science* 252:1162–1164. <http://dx.doi.org/10.1126/science.252.5009.1162>.
 70. Rose A, Meier I. 2004. Scaffolds, levers, rods and springs: diverse cellular functions of long coiled-coil proteins. *Cell. Mol. Life Sci.* 61:1996–2009. <http://dx.doi.org/10.1007/s00018-004-4039-6>.
 71. Lin L, Thanbichler M. 2013. Nucleotide-independent cytoskeletal scaffolds in bacteria. *Cytoskeleton* 70:409–423. <http://dx.doi.org/10.1002/cm.21126>.